Les Cahiers du GERAD ISSN: 0711–2440

Multi-fidelity approaches for general constrained Bayesian optimization with application to aircraft design

O. Cordelier, Y. Diouane, N. Bartoli, É. Laurendeau

G–2026–17

March 2026

La publication de ces rapports de recherche est rendue possible grâce au soutien de HEC Montréal, Polytechnique Montréal, Université McGill, Université du Québec à Montréal, ainsi que du Fonds de recherche du Québec – Nature et technologies.

Dépôt légal – Bibliothèque et Archives nationales du Québec, 2026
– Bibliothèque et Archives Canada, 2026

The publication of these research reports is made possible thanks to the support of HEC Montréal, Polytechnique Montréal, McGill University, Université du Québec à Montréal, as well as the Fonds de recherche du Québec – Nature et technologies.

Legal deposit – Bibliothèque et Archives nationales du Québec, 2026
– Library and Archives Canada, 2026

GERAD HEC Montréal
3000, chemin de la Côte-Sainte-Catherine
Montréal (Québec) Canada H3T 2A7

Tél. : 514 340-6053
Téléc. : 514 340-5665
info@gerad.ca
www.gerad.ca

Multi-fidelity approaches for general constrained Bayesian optimization with application to aircraft design

Oihan Cordelier [a, b]

Youssef Diouane [a, b]

Nathalie Bartoli [c, d]

Éric Laurendeau [b]

[a] *GERAD, Montréal (Qc), Canada, H3T 1J4*

[b] *Polytechnique Montréal, Montréal (Qc), Canada, H3T 0A3*

[c] *DTIS, ONERA, Université de Toulouse, 31000, Toulouse, France*

[d] *Fédération ENAC ISAE-SUPAERO ONERA, Université de Toulouse, France*

oihan.cordelier@polymtl.ca
youssef.diouane@polymtl.ca
nathalie.bartoli@onera.fr

March 2026
Les Cahiers du GERAD
G–2026–17

Abstract : Aircraft design relies heavily on solving challenging and computationally expensive Multidisciplinary Design Optimization problems. In this context, there has been growing interest in multi-fidelity models for Bayesian optimization to improve the MDO process by balancing computational cost and accuracy through the combination of high- and low-fidelity simulation models, enabling efficient exploration of the design process at a minimal computational effort. In the existing literature, fidelity selection focuses only on the objective function to decide how to integrate multiple fidelity levels, balancing precision and computational cost using variance reduction criteria. In this work, we propose novel multi-fidelity selection strategies. Specifically, we demonstrate how incorporating information from both the objective and the constraints can further reduce computational costs without compromising the optimality of the solution. We validate the proposed multi-fidelity optimization strategy by applying it to four analytical test cases, showcasing its effectiveness. The proposed method is used to efficiently solve a challenging aircraft wing aero-structural design problem. The proposed setting uses a linear vortex lattice method and a finite element method for the aerodynamic and structural analysis respectively. We show that employing our proposed multi-fidelity approach leads to 86% to 200% more constraint compliant solutions given a limited budget compared to the state-of-the-art approach.

Keywords: Multidisciplinary design optimization; multi-fidelity Bayesian optimization; fidelity selection; constrained optimization; aero-structural design

Résumé : La conception avion repose en grande partie sur la résolution de problèmes d'optimisation multidisciplinaire complexes et coûteux en termes de calcul. C'est dans ce contexte qu'un intérêt se développe pour les modèles multifidélités appliqués à l'optimisation bayésienne, afin d'améliorer les processus de MDO. L'objectif est de trouver un équilibre entre coût de calcul et précision grâce à la combinaison de modèles de simulation à haute et à basse fidélité, ce qui permet une exploration efficace du processus de conception avec un effort de calcul minimal. Dans la littérature existante, la sélection de la fidélité s'appuie principalement sur la fonction objectif pour décider comment intégrer plusieurs niveaux de fidélité, en équilibrant précision et coût de calcul à l'aide d'un critère de réduction de variance. Dans ce travail, nous proposons de nouvelles stratégies de sélection multifidélité. Plus précisément, nous démontrons comment l'intégration d'informations provenant à la fois de l'objectif et des contraintes peut réduire davantage les coûts de calcul sans compromettre l'optimalité de la solution. Nous validons la stratégie d'optimisation multifidélité proposée en l'appliquant à quatre cas de tests analytiques, démontrant ainsi son efficacité. La méthode proposée est utilisée pour résoudre efficacement un problème complexe de conception aérostructurelle d'aile d'avion. Le cadre proposé utilise une méthode VLM et une méthode des éléments finis pour l'analyse aérodynamique et structurelle respectivement. Nous démontrons que l'utilisation de l'approche multifidélité proposée permet d'obtenir, pour un budget donné, entre 86 % et 200 % plus de solutions respectant les contraintes par rapport à l'approche de l'état de l'art.

Mots clés : Optimisation de conception multidisciplinaire; optimisation bayésienne multifidélité; sélection de fidélité; optimisation contrainte; conception aérostructurelle

1 Introduction

Multidisciplinary Design Optimization (MDO) Raymer (2018) aims to find the best design by considering the trade-offs and dependencies between disciplines (e.g., aerodynamics, structural mechanics, and thermodynamics). Multidisciplinary Design Analysis (MDA) is the study of interacting disciplines, where a design variable of a discipline might influence another. MDO builds upon MDA by incorporating it into an optimization process. Multi-fidelity models also play a crucial role in balancing the accuracy and computational efficiency of MDO across the disciplines. High-fidelity models, such as Reynolds-Averaged Navier-Stokes (RANS), are used to accurately simulate complex flow phenomena, but their computational cost makes them suitable for the final stages of MDO when precision is critical. Euler equations, as medium-fidelity models, simplify certain aspects, such as ignoring viscosity, to reduce computational effort while maintaining reasonable accuracy, which is ideal for intermediate stages (e.g., induced drag). Low-fidelity models, such as those based on Laplace equation (e.g., incompressible flows) provide quick approximations based on simplified assumptions, allowing for rapid exploration of design options across disciplines. By strategically using these models within MDO, designers can efficiently explore and optimize complex designs while ensuring that computational efforts are used effectively.

MDO problems can be formulated as a computationally expensive-to-evaluate blackbox constrained optimization of the form

$$\begin{aligned} \min_{\mathbf{x}\in\mathbb{R}^d} \quad & f(\mathbf{x}) \\ \text{s.t.} \quad & \boldsymbol{g}(\mathbf{x}) \leq \mathbf{0} \\ & \boldsymbol{h}(\mathbf{x}) = \mathbf{0} \end{aligned} \tag{1}$$

where $f : \mathbb{R}^d \mapsto \mathbb{R}$ is the objective function, $\boldsymbol{g} : \mathbb{R}^d \mapsto \mathbb{R}^m$ gives the m inequality constraints, and $\boldsymbol{h} : \mathbb{R}^d \mapsto \mathbb{R}^p$ gives the p equality constraints. The design space $\Omega \subset \mathbb{R}^d$ is a bounded domain. The functions f, $\boldsymbol{g}$ and $\boldsymbol{h}$ are typically simulations with no exploitable properties such as structure or derivatives (i.e., blackbox). Calling f, $\boldsymbol{g}$, and $\boldsymbol{h}$ is often expected to be very computationally expensive and thus takes a long time to evaluate. In this paper, we assume access to multiple sources of fidelity data related to the objective function f and the constraint functions $\boldsymbol{g}$ and $\boldsymbol{h}$. The fidelity levels are assumed to range from the lowest fidelity (cheapest) to the highest fidelity (most expensive). Examples of challenging blackbox MDO problems are commonly encountered in the aerospace industry. See, for instance, Priem et al. (2020b), where Bombardier presents an aircraft optimization use case to identify configurations from early-stage concepts to detailed aircraft designs.

Bayesian Optimization (BO) Frazier (2018); Priem et al. (2020a) is a powerful strategy for solving expensive blackbox problems as in Eq. (1). The use of multiple fidelities to improve BO was explored both for mono-objective Meliani et al. (2019) and multi-objective Charayron et al. (2023) optimization. These latest BO approaches are largely based on powerful multi-fidelity modeling tools of Kennedy (2000). Building on this foundation, Forrester et al. (2007) proposed a multi-fidelity extension for an unconstrained BO strategy, known as the Efficient Global Optimization (EGO) algorithm. Later, EGO was extended to the constrained setting with the development of the *Super EGO* framework (SEGO) Sasena et al. (2002). Meliani et al. (2019) proposed MFSEGO, an extension of SEGO to the multi-fidelity setting. In Meliani et al. (2019); Charayron et al. (2023), a fidelity selection criterion focusing solely on the objective function was introduced to decide how to integrate multiple fidelity levels. The fidelity models related to the constraints did not influence the multi-fidelity optimization strategy. Other multi-fidelity optimization frameworks exist, including MFSKO Huang et al. (2006) and NM2-BO Di Fiore and Mainini (2024); however, they provide limited discussion on constraint-handling strategies. MFSKO proposes possible ideas to integrate constraints but does not provide benchmark results. NM2-BO addresses constraints by reformulating them as penalty terms added to the objective function. Frameworks such as VF-EI Zhang et al. (2018) and VF-PI Ruan et al. (2020) explicitly integrate multi-fidelity constraints, but they cannot efficiently treat equality constraints as they penalize their respective acquisition function using the probability-of-feasibility Schonlau (1997).

In this paper, we investigate the potential of incorporating multiple fidelity levels for constraints, in addition to those related to the objective function, into the optimization process. These range from the most optimistic approach, where decisions are based mainly on the best affordable fidelity level, to the most pessimistic approach, where decisions are guided by the worst affordable fidelity level. The proposed approaches are then used to solve a bi-fidelity aero-structural wing optimization case. The obtained results suggest that taking into account both the objective and constraint functions when deciding the level of fidelity to be used within the optimization process is beneficial; the pessimistic strategy appears to perform best in our tests.

The outline of the paper is as follows. In Section 2, we provide a detailed review of multi-fidelity Gaussian processes. Section 3 reviews BO and its multi-fidelity extension, MFSEGO. Our proposed methodology is introduced in Section 4, where we present a detailed analysis of the properties of the proposed algorithm. Section 5 discusses implementation details and presents the results obtained from four challenging analytical test cases. The results are compared against two other multi-fidelity frameworks, VF-EI and VF-PI. Results from a wing aerostructural design optimization case are also provided. Finally, conclusions and ongoing work are summarized in Section 6.

2 Multi-fidelity Gaussian processes

2.1 Gaussian processes

Gaussian Processes (GP) Rasmussen and Williams (2008) build surrogate models capable of predicting function y values and the corresponding uncertainty of the prediction across its domain from a limited number of function samples. Using Sacks et al. (1989) formulation, the function is modeled following a linear interpolation and a stochastic process, which captures the departure from said linear model as written:

$$y(\boldsymbol{x}) = \sum_{k=1}^{q} \beta_k f_k(\boldsymbol{x}) + Z(\boldsymbol{x}) \tag{2}$$

where $f_k(\boldsymbol{x})$ are q basis functions, and β_k are their corresponding weights. $Z(\boldsymbol{x})$ is characterized by a covariance function:

$$\operatorname{cov}\left[Z(\boldsymbol{x}^i),\ Z(\boldsymbol{x}^j)\right] = \sigma_z^2 R\left(Z(\boldsymbol{x}^i), Z(\boldsymbol{x}^j)\right) = \sigma_z^2 \prod_{l=1}^{d} \exp\left(-\theta_l \left|x_l^i - x_l^j\right|^2\right), \tag{3}$$

where R is the squared exponential correlation function for $\boldsymbol{x}^i$ and $\boldsymbol{x}^j$ two points in $\mathbb{R}^d$. The scale factor σ_z and the vector of d-dimensions $\boldsymbol{\theta}$ correspond to the prior variance and the correlation lengths θ_l in each dimension Rasmussen and Williams (2008).

The Design of Experiments (DoE), denoted as $\text{DoE} = \{(\boldsymbol{x}, y)_k\}_{k=1,\dots,N}$, gathers N samples from the function y from which it is then possible to approximate the hyperparameters by using the Maximum Likelihood Estimation (MLE) Bachoc (2013) and compute vectors and matrices at a query point $\boldsymbol{x}$:

$$\begin{aligned}
\boldsymbol{f}(\boldsymbol{x}) &= (f_1(\boldsymbol{x}), \dots, f_q(\boldsymbol{x}))^\top \in \mathbb{R}^q \\
\boldsymbol{r}(\boldsymbol{x}) &= (R(\boldsymbol{x}_1, \boldsymbol{x}), \dots, R(\boldsymbol{x}_N, \boldsymbol{x}))^\top \in \mathbb{R}^N \\
\boldsymbol{\beta} &= (\beta_1, \dots, \beta_q)^\top \in \mathbb{R}^q \\
\boldsymbol{X} &= (\boldsymbol{x}_1, \dots, \boldsymbol{x}_N)^\top \in \mathbb{R}^{N \times d} \\
\boldsymbol{Y} &= (y_1, \dots, y_N)^\top \in \mathbb{R}^N \\
\boldsymbol{F} &= (\boldsymbol{f}(\boldsymbol{x}_1), \dots, \boldsymbol{f}(\boldsymbol{x}_N))^\top \in \mathbb{R}^{N \times q} \\
\boldsymbol{R} &= R(\boldsymbol{x}, \tilde{\boldsymbol{x}})_{\boldsymbol{x}, \tilde{\boldsymbol{x}} \in \boldsymbol{X}} \in \mathbb{R}^{N \times N}.
\end{aligned} \tag{4}$$

The posterior mean μ and variance σ^2 can be thought of as the surrogate model's prediction and the corresponding uncertainty, and can be expressed as follows:

$$\begin{aligned} \mu(\boldsymbol{x}) &= \boldsymbol{f}(\boldsymbol{x})^\top \boldsymbol{\beta} + \boldsymbol{r}(\boldsymbol{x})^\top \boldsymbol{R}^{-1}(\boldsymbol{Y} - \boldsymbol{F}\boldsymbol{\beta}) \\ \sigma^2(\boldsymbol{x}) &= \sigma_z^2 \left(1 - \boldsymbol{r}(\boldsymbol{x})^\top \boldsymbol{R}^{-1} \boldsymbol{r}(\boldsymbol{x})\right). \end{aligned} \tag{5}$$

2.2 Multi-fidelity Gaussian processes

The accuracy of numerical simulation outputs is often achieved at the expense of increased computational costs. Nevertheless, faster approximations using a coarser mesh, less complex models, or entirely different physical models can provide useful information, such as overall trends in the domain. Kennedy and O'Hagan Kennedy (2000) proposed the formulation presented here:

$$y_{HF}(\boldsymbol{x}) = \rho y_{LF}(\boldsymbol{x}) + \delta(\boldsymbol{x}) \quad \text{s.t.} \quad y_{LF} \perp \delta. \tag{6}$$

The high-fidelity output is expressed as the low-fidelity output scaled by a factor ρ, plus a discrepancy function δ. The discrepancy function is modeled by a Gaussian process with the task of capturing the difference between 2 sequential levels of fidelity. Following this approach, Le Gratiet (2013) proposed a formulation where the LF surrogate model $\hat{y}_{LF}$ is used as a basis function to construct the HF surrogate model $\hat{y}_{HF}$ as follows:

$$\hat{y}_{HF}(\boldsymbol{x}) = \sum_{k=1}^{q} \beta_k f_k(\boldsymbol{x}) + \beta_\rho \hat{y}_{LF}(\boldsymbol{x}) + \delta(\boldsymbol{x}). \tag{7}$$

This formulation can be extended to L levels. This model is built recursively, starting from the lowest level to the highest. Each level ℓ is defined by their respective process variance $\sigma_{z,\ell}$, correlation length $\boldsymbol{\theta}_\ell$, and training data $\boldsymbol{D}_\ell$. Instead of using a single kernel that aggregates the spatial correlation of all levels, one kernel $R_\ell \in \mathbb{R}^{N_\ell \times N_\ell}$ is constructed for each level. Here, N_ℓ represents the number of samples of a given fidelity ℓ. This formulation requires the use of a nested DoE : the sample locations of a given level must be present in all lower DoE ($\boldsymbol{D}_\ell \subseteq \boldsymbol{D}_{\ell-1}$). The mean and variance predictions at a query point $\boldsymbol{x}$ and fidelity level $\ell \geq 2$ are given respectively by:

$$\mu_\ell(\boldsymbol{x}) = \rho_{\ell-1}(\boldsymbol{x})\mu_{\ell-1}(\boldsymbol{x}) + \boldsymbol{f}_\ell(\boldsymbol{x})^\top \boldsymbol{\beta}_\ell + \boldsymbol{r}_\ell(\boldsymbol{x})^\top \boldsymbol{R}_\ell^{-1}\Big(\boldsymbol{Y}_\ell - \rho_{\ell-1}(\boldsymbol{D}_\ell) \odot \boldsymbol{Y}_{\ell-1}(\boldsymbol{D}_\ell) - \boldsymbol{f}_\ell(\boldsymbol{D}_\ell)^\top \boldsymbol{\beta}_\ell\Big) \tag{8}$$

$$\sigma_\ell^2(\boldsymbol{x}) = \rho_{\ell-1}^2(\boldsymbol{x})\sigma_{\ell-1}^2(\boldsymbol{x}) + \underbrace{\sigma_{z,\ell}^2 \left(1 - \boldsymbol{r}_\ell(\boldsymbol{x})^\top \boldsymbol{R}_\ell^{-1} \boldsymbol{r}_\ell(\boldsymbol{x})\right)}_{\sigma_{\delta,\ell}^2}. \tag{9}$$

In this paper, the regression function is constant $\boldsymbol{f}_\ell(\boldsymbol{x}) \to f_\ell = 1$, the scaling factor is a scalar value $\rho_\ell(\boldsymbol{x}) \to \rho_\ell$ and $r_\ell(\boldsymbol{x})$ is the correlation matrix between the training points $\boldsymbol{D}_\ell$ and the query point $\boldsymbol{x}$: $\boldsymbol{r}_\ell(\boldsymbol{x}) = R(\tilde{\boldsymbol{x}}, \boldsymbol{x})_{\tilde{\boldsymbol{x}} \in \boldsymbol{D}_\ell}$. $\rho_{\ell-1}(\boldsymbol{D}_\ell)$ and $\boldsymbol{Y}_{\ell-1}(\boldsymbol{D}_\ell)$ denote the scaling factors and function values of the previous level for points in $\boldsymbol{D}_{\ell-1}$ and $\boldsymbol{D}_\ell$. The previous level function values are present in the previous and current level DOE. The mean and variance prediction functions for $\ell = 1$ reduce to Eq. (5). The model parameters $\{\boldsymbol{\beta}_\ell, \sigma_{z,\ell}, \boldsymbol{\theta}_\ell\}_{\ell=1}^{L}$, as well as the scaling factors $\{\rho_\ell\}_{\ell=1}^{L-1}$, are estimated by maximizing the restricted log-likelihood sequentially, starting from the lowest level to the highest. Once the hyper-parameters of a given level are estimated, they are held fixed for the subsequent levels. The variance contribution of a given level ℓ scaled up to the highest level L can be computed using:

$$\sigma_{\text{cont}}^2(\ell, \boldsymbol{x}) = \sigma_{\delta,\ell}^2(\boldsymbol{x}) \prod_{j=\ell}^{L-1} \rho_j^2 \tag{10}$$

This multi-fidelity GP formulation is used to construct surrogate models for the objective and the constraint functions employed in the Bayesian optimization approach discussed in Sections 3 and 4.

3 Multi-fidelity Bayesian optimization

3.1 Bayesian optimization

Constrained Bayesian optimization employs Gaussian processes to model both the objective and constraint functions. At the beginning of the optimization process, the initial models are constructed using a limited number of function samples. At a given iteration i, the next sampling location is selected by optimizing an acquisition function α:

$$\begin{aligned} \boldsymbol{x}_i \in \underset{\boldsymbol{x} \in \mathbb{R}^d}{\arg\max} \quad & \alpha(\boldsymbol{x}) \\ \text{s.t.} \quad & \boldsymbol{\mu}_g(\boldsymbol{x}) \leq \mathbf{0} \\ & \boldsymbol{\mu}_h(\boldsymbol{x}) = \mathbf{0} \end{aligned} \tag{11}$$

where $\boldsymbol{\mu}_g(\boldsymbol{x})$ and $\boldsymbol{\mu}_h(\boldsymbol{x})$ are the mean predictions of the inequality and equality constraints. The SEGO framework Sasena et al. (2002) utilizes the Expected Improvement (EI) function Močkus (1975) as an acquisition function denoted by:

$$\alpha(x) = \mathrm{EI}(\boldsymbol{x}) = \begin{cases} (f_{\min} - \mu_f(\boldsymbol{x}))\Phi\left(\frac{f_{\min} - \mu_f(\boldsymbol{x})}{\sigma_f(\boldsymbol{x})}\right) + \sigma_f(\boldsymbol{x})\phi\left(\frac{f_{\min} - \mu_f(\boldsymbol{x})}{\sigma_f(\boldsymbol{x})}\right) & \text{if } \sigma_f(\boldsymbol{x}) > 0 \\ 0 & \text{if } \sigma_f(\boldsymbol{x}) = 0 \end{cases} \tag{12}$$

The output mean $\mu_f(\boldsymbol{x})$ and variance $\sigma_f^2(\boldsymbol{x})$ of the objective GP are used to identify locations with probabilities of improving the current best feasible minimum objective sampled value $f_{\min}$. If no point is feasible, the objective value with the least constraint violation is used instead. Φ and ϕ are, respectively, the cumulative distribution and the probability density functions of $\mathcal{N}(0,1)$. The blackbox functions are sampled at the infill location $\boldsymbol{x}_i$ and the corresponding objective and constraint data are added to the DoE. Even if the sampled point is unfeasible, it is still added to the GP training points to improve the accuracy of the objective and constraints GPs. This process is repeated until a convergence criterion is met, such as a maximum number of iterations. The SEGO framework is summarized by Algorithm 1.

Algorithm 1 The Super Efficient Global Optimization (SEGO) framework.

Input: Design space Ω, objective and constraints oracles $\{f, \boldsymbol{g}, \boldsymbol{h}\}$, and budget, i.e., max_iter.
Output: $f_{\min}$ the best feasible point in terms of the objective function f.
Generate an initial DoE;
Set $f_{\min}$ to the best feasible point in terms of the objective function f;
$i \leftarrow 0$;
while $i \leq$ max_iter **do**
  Build the surrogate models using GPs for the objective and constraint functions;
  $\boldsymbol{x}_i \in \underset{\boldsymbol{x} \in \Omega}{\arg\max}\{\alpha(\boldsymbol{x}) \quad \text{s.t.} \quad \boldsymbol{\mu}_g(\boldsymbol{x}) \leq \mathbf{0},\ \boldsymbol{\mu}_h(\boldsymbol{x}) = \mathbf{0}\}$; ▷ Find infill location
  Evaluate f, $\boldsymbol{g}$ and $\boldsymbol{h}$ at $\boldsymbol{x}_i$;
  Update the DoE;
  Set $f_{\min}$ to the best feasible point in terms of the objective function f;
  $i \leftarrow i + 1$;
end while

3.2 Bayesian optimization with only objective multi-fidelity selection criteria

Multi-fidelity Bayesian optimization leverages multiple levels of fidelity to reduce the cost of optimization and increase the precision of the surrogate models with computationally cheaper data. The MFSEGO framework employed in Meliani et al. (2019); Charayron et al. (2023) is heavily derived from the SEGO framework previously discussed. The objective and constraint functions are modeled using the Le Gratiet Multi-Fidelity Kriging model, thus requiring a nested DoE such that $\mathrm{DoE}_\ell \subseteq \mathrm{DoE}_{\ell-1}$ for $\ell = 2, \ldots, L$. The infill location and the fidelity level at which to sample said location are computed sequentially as a two-step approach. For the first step, the infill location is selected using an acquisition function such as EI Močkus (1975) or the scaled WB2 Bartoli et al. (2019). $f_{\min}$ corresponds to

the best feasible objective evaluated at the highest level of fidelity. From Eq. (10), the reduction in variance of the surrogate model, if the function were to be sampled at level ℓ for the objective function f, can be computed as follows:

$$\sigma^2_{(\text{red},0)}(\ell, \boldsymbol{x}_i) = \sum_{\ell'=1}^{\ell} \sigma^2_{(\text{cont},0)}(\ell', \boldsymbol{x}_i) = \sum_{\ell'=1}^{\ell} \sigma^2_{(0,\delta,\ell')}(\boldsymbol{x}_i) \prod_{j=\ell'}^{L-1} \rho^2_{(j,0)}. \tag{13}$$

The subscript $(\text{red}, 0)$ indicates that the reduction is related to the objective function. The nested DoE requires that if the function is sampled at fidelity ℓ, it must also be sampled at all lower fidelity levels. The total cost of sampling a level is given by $\sum_{\ell'=1}^{\ell} c_{\ell'}$ where $c_{\ell'}$ represents the individual cost of each level ℓ' for evaluating the objective and constraint functions. To select the fidelity level for the second step, we use the best ratio of variance reduction to the cost squared:

$$\ell_i^{\text{obj}} = \underset{\ell \in \{1,\dots,L\}}{\arg\max} \frac{\sigma^2_{(\text{red},0)}(\ell, \boldsymbol{x}_i)}{\left(\sum_{\ell'=1}^{\ell} c_{\ell'}\right)^2}. \tag{14}$$

Meliani et al. (2019) suggest that the cost should be squared, since the variances are scaled with the squared scaling factor.

4 MFSEGO using both objective and constraints multi-fidelity criteria

Previous work only applied the fidelity criterion to the objective surrogate model, e.g., Meliani et al. (2019); Charayron et al. (2023). Since constraints can also be modeled using different fidelity levels, in this section, three other fidelity criteria are proposed to incorporate the variances of the constraint models into the fidelity level selection process. The fidelity criterion previously discussed (see Eq. (14)) will be referred to as the "objective-only" fidelity criterion.

Inspired by Eq. (13), for a given $k \in \{0, \dots, m+p\}$, the reduction in variance of the k-th GP component is given by

$$\sigma^2_{(\text{red},k)}(\ell, \boldsymbol{x}_i) = \sum_{\ell'=1}^{\ell} \sigma^2_{(\text{cont},k)}(\ell', \boldsymbol{x}_i) = \sum_{\ell'=1}^{\ell} \sigma^2_{(k,\delta,\ell')}(\boldsymbol{x}_i) \prod_{j=\ell'}^{L-1} \rho^2_{(j,k)}. \tag{15}$$

Let $\sigma^2_{(\text{norm},k)}$ be the normalized reduction in variance of g_k with respect to the cost:

$$\sigma^2_{(\text{norm},k)}(\ell, \boldsymbol{x}_i) = \sigma^2_{(\text{red},k)}(\ell, \boldsymbol{x}_i) \left(\sum_{\ell'=1}^{\ell} c_{\ell'}\right)^{-2}. \tag{16}$$

The "Average" variance reduction criterion averages the variance reduction of the objective and constraint models for a level k and divides it by the level's total cost squared. The level with the best ratio is selected. This approach can be extended to $m+p+1$ GPs (one GP model for the objective function and $m+p$ GPs for the constraints) as written:

$$\ell_i^{\text{avg}} = \underset{\ell \in \{1,\dots,L\}}{\arg\max} \sum_{k=0}^{m+p} \sigma^2_{(\text{norm},k)}(\ell, \boldsymbol{x}_i). \tag{17}$$

The "Optimistic" variant computes the best level $\ell_i^{\min}$ for each GP and selects the overall lowest from the $m+p+1$ GPs:

$$\ell_i^{\min} = \min_{k \in \{0,\dots,m+p\}} \left(\underset{\ell \in \{1,\dots,L\}}{\arg\max}\, \sigma^2_{(\text{norm},k)}(\ell, \boldsymbol{x}_i) \right). \tag{18}$$

The third variant, referred to as the "Pessimistic" one, computes the overall highest level from the $m+p+1$ GPs:

$$\ell_i^{\max} = \max_{k\in\{0,\dots,m+p\}} \left(\arg\max_{\ell\in\{1,\dots,L\}} \sigma^2_{(\text{norm},k)}(\ell, \boldsymbol{x}_i) \right). \tag{19}$$

The MFSEGO framework using both objective and constraints multi-fidelity criteria is given by Algorithm 2, where f represents the objective function, $\boldsymbol{g}$ the inequality constraint functions, and $\boldsymbol{h}$ the equality constraint functions.

Algorithm 2 The multi-fidelity based SEGO (MFSEGO) for constrained optimization.

Input: Design space Ω, objective and constraints oracles per fidelity level $\{f, \boldsymbol{g}, \boldsymbol{h}\}_{\ell\in\{1,\dots,L\}}$, cost per fidelity level $\{c_\ell\}_{(\ell\in\{1,\dots,L\})}$, and a budget, i.e., max_iter.
Output: $f_{\min}$ the best feasible point in terms of the high-fidelity objective value.
Generate an initial nested $\{\text{DoE}_\ell\}_{\ell\in\{1,\dots,L\}}$;
Set $f_{\min}$ to the best feasible point in terms of the objective function in $\text{DoE}_{\ell=L}$;
$i \leftarrow 0$;
while $i \leq$ max_iter **do**
  Build GPs for the objective and the constraints;
  $\boldsymbol{x}_i \in \arg\max_{\boldsymbol{x}\in\Omega}\{\alpha(\boldsymbol{x}) \quad \text{s.t.} \quad \boldsymbol{\mu}_g(\boldsymbol{x}) \leq \boldsymbol{0},\ \boldsymbol{\mu}_h(\boldsymbol{x}) = \boldsymbol{0}\}$; ▷ Find infill location
  Select a fidelity level $\ell_i \in \{\ell_i^{\text{obj}}, \ell_i^{\text{avg}}, \ell_i^{\min}, \ell_i^{\max}\}$;
  for ℓ' in $\{1,\dots,\ell_i\}$ **do** ▷ Sample and update each fidelity level up to ℓ_i
    Evaluate the objective and constraints at $\boldsymbol{x}_i$;
    Update the nested $\text{DoE}_{\ell'}$;
  end for
  Update $f_{\min}$ as the best feasible point in terms of the objective value in $\text{DoE}_{\ell=L}$;
  $i \leftarrow i+1$
end while

5 Numerical results

5.1 Implementations details

All surrogate models are built using the MFK model implemented in the SMT package Saves et al. (2024). The GP hyperparameters are estimated by maximizing the restricted log-likelihood. The optimized hyperparameters from the previous iteration are used as a starting location for the sub-optimization problem in addition to $3d$ other starting locations generated using LHS. The constrained acquisition function is optimized using SLSQP Kraft (1988) because of its ability to handle both inequality and equality constraints. A multi-start strategy is used to escape any local minima. The starting locations are generated using LHS. As the number of infill samples increases, the output variance of the objective surrogate model tends to decrease. The gradient of EI can quickly fall under the machine epsilon ϵ, making it practically difficult to optimize numerically. To address this issue, Ament et al. Ament et al. (2023) proposed a numerically stable implementation of the Log Expected Improvement acquisition function as denoted by:

$$\alpha(\boldsymbol{x}) = \log \text{EI}(\boldsymbol{x}) = \texttt{log\_h}\left(\frac{f_{\min} - \mu_f(\boldsymbol{x})}{\sigma_f(\boldsymbol{x})}\right) + \log(\sigma_f(\boldsymbol{x})) \tag{20}$$

where

$$\texttt{log\_h}(z) = \begin{cases} \log(\phi(z) + z\Phi(z)) & z > -1 \\ -\frac{z^2}{2} - c_1 + \texttt{log1mexp}(\log(\texttt{erfcx}(-z/\sqrt{2})|z|) + c_2) & -1/\sqrt{\epsilon} < z \leq -1 \\ -\frac{z^2}{2} - c_1 - 2\log(|z|) & z \leq -1/\sqrt{\epsilon} \end{cases}$$

with $c_1 = \frac{1}{2}\log(2\pi)$, $c_2 = \frac{1}{2}\log(\pi/2)$ and $\epsilon > 0$ is set to the epsilon machine tolerance. The functions `log1mexp` and `erfcx` are defined as $\texttt{log1mexp}(z) = \log(1-\exp(z))$ and $\texttt{erfcx}(z) = \exp(z^2)\,\text{erfc}(z)$.

This log EI function returns non-numerically zero values even when the probability of improvement would lead traditional EI to fall below epsilon. Furthermore, when the output variances of the GPs decrease, so does the variance reduction σ^2_{red}. To avoid $\sigma^2_{(\text{norm},k)}$ falling below machine epsilon, the cost of every level $c_{\ell=\{1,\dots,L\}}$ is normalized by the highest level $c_{\ell=L}$.

5.2 Results on analytical test problems

The MFSEGO algorithm, as described in Sections 2 and 3, is applied to multi-fidelity constrained problems: the Rosenbrock problem (noted MF Rosenbrock) Lam et al. (2015), the Branin problem (noted MF Branin) Qian et al. (2021), the Sasena problem (noted MF Sasena) Qian et al. (2021), and the Gano problem (noted MF Gano) Gano et al. (2005). Table 1 summarizes the test problem characteristics. The respective objective and constraint functions are given in Appendix A.1. The objective and constraint functions are each defined with two fidelity levels. The LF functions are obtained by adding a perturbation to their HF counterpart. The global minimum of each problem is located on the constraint's boundary. A set of 25 initial feasible DoE was created for each problem.

Table 1: Analytical test problems properties.

Problem	Dimensions	Domain	$\min_{\boldsymbol{x}\in\Omega_g} f$	$\arg\min_{\boldsymbol{x}\in\Omega_g} f$	ρ_f	ρ_g	LF DoE	HF DoE
MF Rosenbrock	2	$[-2,\ 2]$	0.1785	$[0.5777,\ 0.3325]$	≈ 1	0.9986	6	3
MF Branin	2	$[0,\ 1]$	5.5757	$[0.9676,\ 0.2067]$	≈ 1	0.8163	6	3
MF Sasena	2	$[0,\ 5]$	-1.1743	$[2.7450,\ 2.3523]$	0.3513	0.2981	6	3
MF Gano	2	$[0.1, 10]$	5.6684	$[0.8842, 1.1507]$	≈ 1	0.9723	6	3

Figure 1 compares MFSEGO with SEGO and two other multi-fidelity constrained BO frameworks: VF-EI Zhang et al. (2018) and VF-PI Ruan et al. (2020). These two approaches do not require the use of a nested DoE. To handle the constraints when maximizing their respective acquisition function, both frameworks penalize it with the probability-of-feasibility (PoF) Schonlau (1997). This method is not well suited for handling multiple constraints as it often drives the acquisition function to be numerically zero over the feasible domain and cannot efficiently handle equality constraints. Furthermore, both frameworks were implemented with the MFCK model in the SMT package, as it supports non-nested DoE. Their acquisition function is maximized using L-BFGS-B Byrd et al. (1995) with a multi-start strategy. Table 2 summarizes the properties of MFSEGO, VF-EI, and VF-PI. All methodologies are available in the BOMA repository.[1] Figure A1 in Appendix A.5 displays the data profile for the same experiments. It illustrates that MFSEGO converges more efficiently than VF-EI and VF-PI. VF-PI is shown to be more efficient than SEGO except for a few instances where it failed to converge.

Table 2: Multi-fidelity framework comparison

Framework	SMT Surrogate	DoE	MF constraint	Equality constraints
MFSEGO	MFK	Nested	Sub-solver	✓
VF-EI	MFCK	Non-nested	PoF	x
VF-PI	MFCK	Non-nested	PoF	x

Figure 2 compares the fidelity criteria as discussed in Section 3. When applied to the 4 previously mentioned test problems, no fidelity criterion distinguished itself from the others. It should be noted that the Objective-Only criterion corresponds to the state of the art MFSEGO algorithm. Moreover, the difference in the required budget for convergence between the proposed fidelity criteria decreases when using a higher cost ratio.

[1] https://github.com/oihanc/boma

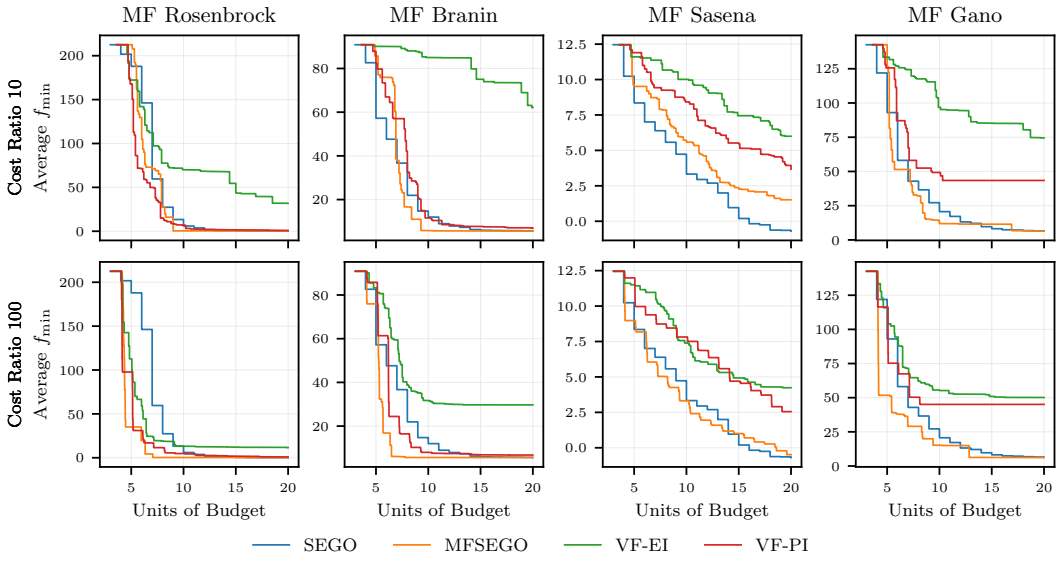

Figure 1: Multi-fidelity BO frameworks comparison. Analytical problems convergence results for the Rosenbrock, Branin, Sasena and Gano problems with two different cost ratios. Each optimization framework was run on 25 DoE.

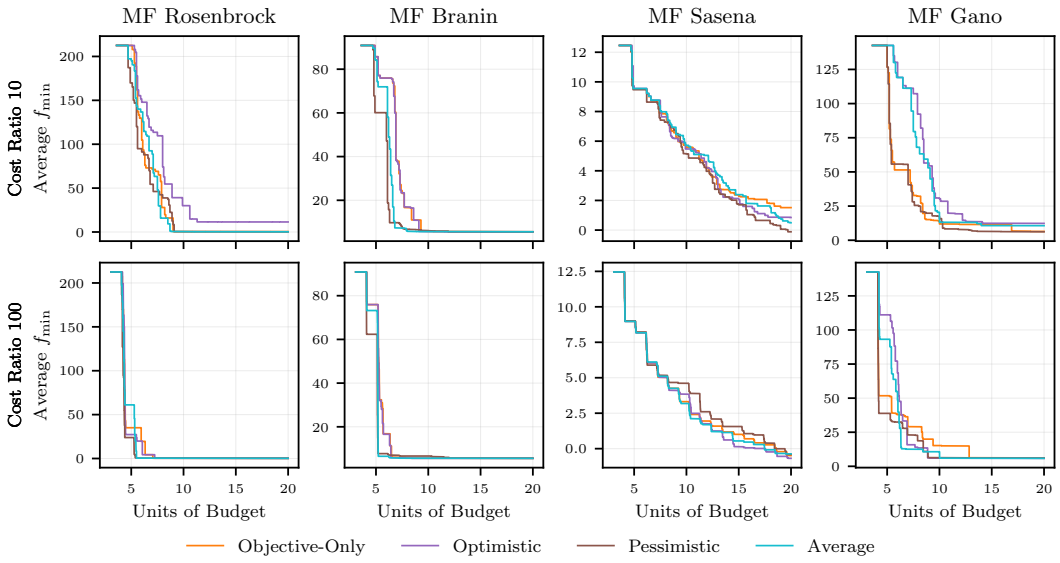

Figure 2: Fidelity criteria comparison. Analytical problems convergence results for the MF Rosenbrock, MF Branin, MF Sasena and MF Gano problems with two different cost ratios. Each fidelity criterion was run on 25 DoE.

5.3 Multi-fidelity aero-structural wing design optimization

The fidelity criteria proposed in Section 3 were benchmarked on a aero-structural test case using OpenAeroStruct Jasa et al. (2018). Table 3 summarizes the problem characteristics. The objective is to minimize the fuel burn using the Breguet equation:

$$\texttt{fuelburn} = (W_0 + W_s)\left(\exp(\frac{RC_T}{aM}\frac{C_D}{C_L}) - 1\right) \tag{21}$$

with regards to the angle-of-attack, the wing twist, and the thickness of the spar. W_0 and W_s respectively symbolize the wing empty weight without fuel and structural elements, and the wing structural weight due to the spar. R corresponds to the aircraft total range; C_T to the specific fuel consumption;

a to the speed of sound and M to the Mach number. Both the wing twist and the spar thickness are defined using 5 control points uniformly distributed along the wing, from which a B-Spline is fitted. Two constraints are imposed: the lift force must be equal to the weight, and the wing structural loads must respect a safety factor of 2.5. It should be noted that the fuel burn objective and the lift-to-weight constraint are well correlated, contrary to the structural failure constraint.

Table 3: Definition of the wing aerostructural optimization problem.

	Function/variable	Description	Quantity	Range	ρ_{Pearson}
Minimize	`fuel_burn`	Fuel Burn	1	–	0.99
with respect to	AoA	Angle-of-Attack [deg]	1	[8, 12]	–
	α_{twist}	Twist [deg]	5	$[-6, 3]$	–
	t_{spar}	Spar thickness [m]	5	[0.0015, 0.05]	–
subject to	$L/W = 1$	Lift-to-Weight ratio	1	–	0.98
	$\sigma_{\text{VM}} \leq 0$	Von-Mises criterion	1	–	0.70

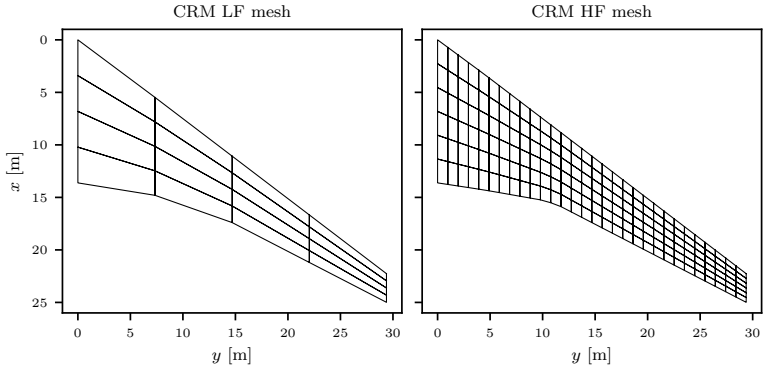

Figure 3: CRM multi-fidelity VLM mesh comparison. The LF and HF meshes use 4×4 panels and 6×30 panels respectively. The cost ratio between the 2 levels is 30.

Figure 3 illustrates the low- and high-fidelity meshes used for this test case. The aerodynamic forces are computed using the Vortex Lattice method (VLM) which assumes an incompressible and inviscid fluid flow. The structural forces are computed with a finite-element method. The 4 fidelity criteria were benchmarked on 25 instances, each starting with a different nested DoE comprised of 122 LF points and 12 HF points. Due to the equality constraint, no initial DoE was feasible. The cost ratio between these fidelities is 30. Using this value led the optimization runs to rarely sample the HF level. Excessive LF sampling increases the BO overhead cost; thus, to encourage more frequent HF evaluations, the cost ratio used in Eq. (16) was reduced to 10.

Figure 4 illustrates data profiles for various absolute constraint tolerance ϵ and relative objective tolerance τ. Here ϵ is defined as the Root Square Constraint Violation (RSCV) defined by:

$$\text{RSCV} = \sqrt{\sum_{i=1}^{m} \max(g_i, 0)^2 + \sum_{j=1}^{p} h_j^2}. \tag{22}$$

Additionally, a run is said to be τ-solved if the following criterion is met:

$$f^i - f_0 \geq (1 - \tau)(f^\star - f_0) \tag{23}$$

where f_0 is the greatest first feasible objective value over all the runs, and $f^\star$ is the best feasible objective value over all the runs.

The Pessimistic criterion clearly outperforms the other fidelity criteria, especially when imposing stricter constraints and objective tolerances. Compared to the state of the art approach using the

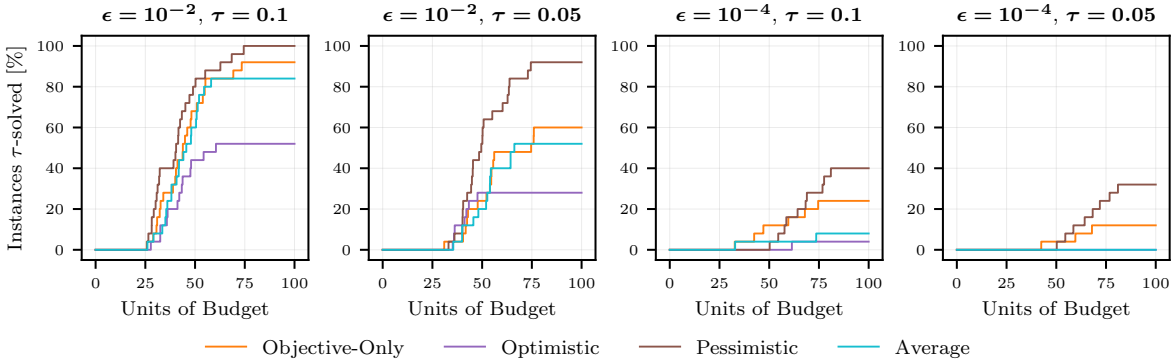

Figure 4: Fidelity criteria comparison on the wing aerostructural optimization problem. ϵ and τ denote the absolute constraint tolerance and the relative objective tolerance respectively. Each fidelity criterion was run on 25 DoE.

Objective-Only criterion, the Pessimistic fidelity criterion solved 9% to 200% more instances, with the difference growing for stricter tolerances. Figure 5 compares the wing twist, the spar thickness, the lift distribution, and the structural safety factor along the wing semispan of the best solution obtained using MFSEGO, and SLSPQ. The corresponding configurations from the initial HF DOE are also shown. As a gradient-based solver, SLSQP requires a single starting point, which was selected as the point with the smallest constraint violation in the HF DOE. Being a mono-fidelity solver, SLSQP operated exclusively on the HF objective and constraint functions. An optimal lift distribution would follow an elliptical shape. In this case, both MFSEGO and SLSQP solutions are limited by the structural constraint.

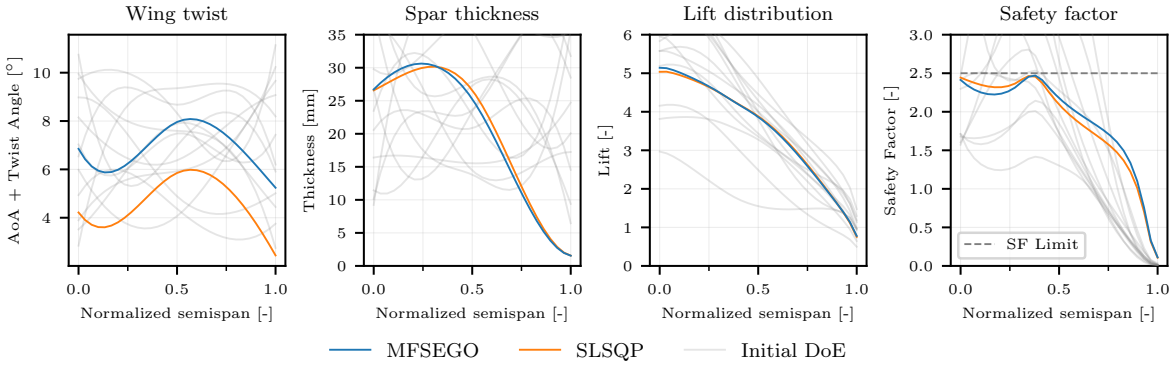

Figure 5: Comparison of the best solutions found with MFSEGO and SLSQP for wing twist, tubular spar thickness, lift distribution and structural safety factor.

6 Conclusions and perspectives

In this paper, we investigate the potential of incorporating multiple fidelity levels for both the constraints and the objective function into a multi-fidelity constrained Bayesian optimization framework, i.e., MFSEGO. Different criteria are considered to handle the multi-fidelity aspects, ranging from the most optimistic approach, where decisions are mainly based on the best affordable fidelity level, to the most pessimistic approach, where decisions are guided by the worst affordable fidelity level.

MFSEGO, VF-EI Zhang et al. (2018), and VF-PI Ruan et al. (2020) were benchmarked on 4 constrained multi-fidelity test problems. SEGO was also benchmarked as a mono-fidelity reference. Overall, MFSEGO proved to be more efficient. Three proposed multi-fidelity criteria were benchmarked against the existing objective-only multi-fidelity criterion and showed comparable performance on the

analytical test problems. However, the pessimistic criterion proved more efficient on the aero-structural wing design problem: for a limited budget and strict tolerances, the pessimistic criterion solved more instances than any other multi-fidelity criterion. Results indicate that multi-fidelity approaches can reduce the computational budget while achieving similar convergence. Future work includes integrating mixed-integer variables and fidelity-dependent design spaces to evaluate the full potential of the MFSEGO approach on a more complex benchmark Saves et al. (2023), such as a test case similar to the Bombardier Research Aircraft Configuration (BRAC) Priem et al. (2020b).

A Appendix

A.1 Rosenbrock analytical test problem

The Rosenbrock multi-fidelity test problem Lam et al. (2015) is defined by:

$$\begin{aligned} f_{HF} &= (1-x_0)^2 + 100(x_1 - x_0^2)^2 \\ f_{LF} &= f_{HF}(x_0, x_1) + 0.1\sin(10x_0 + 5x_1) \\ g_{HF} &= x_0^2 + \sqrt{x_1 - 1} \leq 0 \\ g_{LF} &= g_{HF}(x_0, x_1) - 0.1\sin(10x_0 + 5x_1) \leq 0. \end{aligned} \tag{A1}$$

A.2 Branin analytical test problem

The modified Branin multi-fidelity test problem Qian et al. (2021) is defined by:

$$\begin{aligned} f_{HF} &= \left(15x_1 - \frac{5.1}{4\pi^2}(15x_0 - 5)^2 + \frac{5}{\pi}(15x_0 - 5) - 6\right)^2 \\ &\quad + 10\left(1 - \frac{1}{8\pi}\right)\cos(15x_0 - 5) + 10 + 5x_0 \\ f_{LF} &= f_{HF}(x_0, x_1) - \cos(0.5x_0) - x_1^3 \\ g_{HF} &= -x_0 x_1 + \frac{1}{5} \leq 0 \\ g_{LF} &= -x_0 x_1 + \frac{3}{10}x_0 - \frac{7}{10}x_1 \leq 0. \end{aligned} \tag{A2}$$

A.3 Sasena analytical test problem

The Sasena multi-fidelity test problem Qian et al. (2021) is defined by:

$$\begin{aligned} f_{HF} &= 2 + 0.01(x_1 - x_0^2)^2 + (1 - x_0)^2 + 2(2 - x_1)^2 + 7\sin(x_0)\sin(0.7x_0 x_1) \\ f_{LF} &= f_{HF}(x_0, x_1) + \exp x_0 - x_1^3 \\ g_{HF} &= -\sin(x_0 - x_1 - \pi/8) \leq 0 \\ g_{LF} &= g_{HF}(x_0, x_1) + 0.2x_1 - 0.7x_0 + x_0 x_1 \leq 0. \end{aligned} \tag{A3}$$

A.4 Gano analytical test problem

The Gano multi-fidelity test problem Gano et al. (2005) is defined by:

$$\begin{aligned} f_{HF} &= 4x_1^2 + x_2^3 + x_1 x_2 \\ f_{LF} &= 4(x_1 + 0.1)^2 + (x_2 - 0.1)^3 + x_1 x_2 + 0.1 \\ g_{HF} &= 1/x_1 + 1/x_2 - 2 \leq 0 \\ g_{LF} &= 1/x_1 + 1/(x_2 + 0.1) - 2 - 0.001 \leq 0. \end{aligned} \tag{A4}$$

A.5 Multi-fidelity BO frameworks data profile

Figure A1 aggregates the optimization results displayed in Fig. 1 for the MF Rosenbrock, MF Branin and the MF Gano test functions. The MF Sasena function was excluded due to its poor objective and constraint fidelity correlation factors. In decreasing order of convergence efficiency, the multi-fidelity framework ranking is: MFSEGO, VF-PI, and VF-EI. Given 20 units of budget, only MFSEGO and its mono-fidelity counterpart solved all 75 instances.

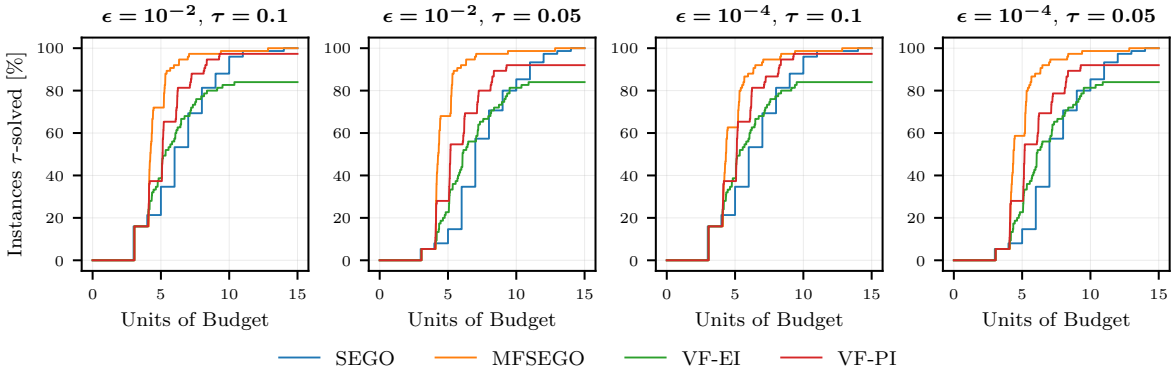

Figure A1: Multi-fidelity BO frameworks comparison. Data profile generated with the MF Rosenbrock, MF Branin and MF Gano test problems with a fixed cost ratio of 100.

References

Sebastian Ament, Samuel Daulton, David Eriksson, Maximilian Balandat, and Eytan Bakshy. Unexpected improvements to expected improvement for bayesian optimization. Advances in Neural Information Processing Systems, 36:20577–20612, 2023. doi: 10.5555/3666122.3667026.

François Bachoc. Cross validation and maximum likelihood estimations of hyper-parameters of gaussian processes with model misspecification. Computational Statistics & Data Analysis, 66:55–69, 2013. doi: 10.48550/arXiv.1301.4320.

N. Bartoli, T. Lefebvre, S. Dubreuil, R. Olivanti, R. Priem, N. Bons, J.R.R.A. Martins, and J. Morlier. Adaptive modeling strategy for constrained global optimization with application to aerodynamic wing design. Aerospace Science and Technology, 90:85–102, 2019. doi: 10.1016/j.ast.2019.03.041.

Richard H. Byrd, Peihuang Lu, Jorge Nocedal, and Ciyou Zhu. A Limited Memory Algorithm for Bound Constrained Optimization. SIAM Journal on Scientific Computing, 16(5):1190–1208, September 1995. doi: 10.1137/0916069.

Rémy Charayron, Thierry Lefebvre, Nathalie Bartoli, and Joseph Morlier. Towards a multi-fidelity & multi-objective Bayesian optimization efficient algorithm. Aerospace Science and Technology, 142:108673, 2023. doi: 10.1016/j.ast.2023.108673.

Francesco Di Fiore and Laura Mainini. NM2-BO: Non-Myopic Multifidelity Bayesian Optimization. Knowledge-Based Systems, 299:111959, September 2024. doi: 10.1016/j.knosys.2024.111959.

Alexander I.J Forrester, András Sóbester, and Andy J Keane. Multi-fidelity optimization via surrogate modelling. Proceedings of the Royal Society. A, Mathematical, physical, and engineering sciences, 463(2088): 3251–3269, 2007. doi: 10.1098/rspa.2007.1900.

Peter I Frazier. A tutorial on bayesian optimization. arXiv:1807.02811, 2018. doi: 10.48550/arXiv.1807.02811.

Shawn E. Gano, John E. Renaud, and Brian Sanders. Hybrid Variable Fidelity Optimization by Using a Kriging-Based Scaling Function. AIAA Journal, 43(11):2422–2433, November 2005. doi: 10.2514/1.12466.

D. Huang, T. T. Allen, W. I. Notz, and R. A. Miller. Sequential kriging optimization using multiple-fidelity evaluations. Structural and Multidisciplinary Optimization, 32(5):369–382, November 2006. doi: 10.1007/s00158-005-0587-0.

John P. Jasa, John T. Hwang, and Joaquim R. R. A. Martins. Open-source coupled aerostructural optimization using Python. Structural and Multidisciplinary Optimization, 57(4):1815–1827, April 2018. doi: 10.1007/s00158-018-1912-8.

M. Kennedy. Predicting the output from a complex computer code when fast approximations are available. Biometrika, 87(1):1–13, 2000. doi: 10.1093/biomet/87.1.1. Number: 1.

D. Kraft. A Software Package for Sequential Quadratic Programming. Technical Report DFVLR-FB 88-28, DLR German Aerospace Center, Germany, 1988.

Rémi Lam, Douglas L. Allaire, and Karen E. Willcox. Multifidelity optimization using statistical surrogate modeling for non-hierarchical information sources. In 56th AIAA/ASCE/AHS/ASC Structures, Structural Dynamics, and Materials Conference. American Institute of Aeronautics and Astronautics, 2015. doi: 10.2514/6.2015-0143.

Loic Le Gratiet. Multi-fidelity Gaussian process regression for computer experiments. PhD thesis, Université Paris-Diderot - Paris VII, 2013.

Mostafa Meliani, Nathalie Bartoli, Thierry Lefebvre, Mohamed-Amine Bouhlel, Joaquim R. R. A. Martins, and Joseph Morlier. Multi-fidelity efficient global optimization: Methodology and application to airfoil shape design. In AIAA Aviation 2019 Forum. American Institute of Aeronautics and Astronautics, 2019. doi: 10.2514/6.2019-3236.

J. Močkus. On bayesian methods for seeking the extremum. In G. I. Marchuk, editor, Optimization Techniques IFIP Technical Conference, pages 400–404. Springer Berlin Heidelberg, 1975. doi: 10.1007/978-3-662-38527-2_55.

R. Priem, N. Bartoli, Y. Diouane, and A. Sgueglia. Upper trust bound feasibility criterion for mixed constrained bayesian optimization with application to aircraft design. Aerospace Science and Technology, 105:105980, 2020a. doi: 10.1016/j.ast.2020.105980.

Remy Priem, Hugo Gagnon, Ian Chittick, Stephane Dufresne, Youssef Diouane, and Nathalie Bartoli. An efficient application of bayesian optimization to an industrial mdo framework for aircraft design. In AIAA AVIATION 2020 FORUM. American Institute of Aeronautics and Astronautics, 2020b. doi: 10.2514/6.2020-3152.

Jiachang Qian, Yuansheng Cheng, Anfu Zhang, Qi Zhou, and Jinlan Zhang. Optimization design of metamaterial vibration isolator with honeycomb structure based on multi-fidelity surrogate model. Structural and Multidisciplinary Optimization, 64(1):423–439, 2021. doi: 10.1007/s00158-021-02891-6.

Carl Edward Rasmussen and Christopher K. I. Williams. Gaussian processes for machine learning. Adaptive computation and machine learning. MIT Press, 3. print edition, 2008.

D. P. Raymer. Aircraft Design: A Conceptual Approach, Sixth Edition. Virginia: American Institute of Aeronautics & Astronautics, 2018.

Xiongfeng Ruan, Ping Jiang, Qi Zhou, Jiexiang Hu, and Leshi Shu. Variable-fidelity probability of improvement method for efficient global optimization of expensive black-box problems. Structural and Multidisciplinary Optimization, 62(6):3021–3052, December 2020. doi: 10.1007/s00158-020-02646-9.

Jerome Sacks, Susannah B. Schiller, and William J. Welch. Designs for computer experiments. Technometrics, 31(1):41–47, 1989. doi: 10.1080/00401706.1989.10488474. Number: 1.

M. J. Sasena, P. Papalambros, and P. Goovaerts. Exploration of metamodeling sampling criteria for constrained global optimization. Engineering optimization, 34:263–278, 2002. doi: 10.1080/03052150211751.

P. Saves, Y. Diouane, N. Bartoli, T. Lefebvre, and J. Morlier. A mixed-categorical correlation kernel for Gaussian process. Neurocomputing, 550:126472, 2023. doi: 10.1016/j.neucom.2023.126472.

Paul Saves, Rémi Lafage, Nathalie Bartoli, Youssef Diouane, Jasper Bussemaker, Thierry Lefebvre, John T. Hwang, Joseph Morlier, and Joaquim R.R.A. Martins. SMT 2.0: A surrogate modeling toolbox with a focus on hierarchical and mixed variables gaussian processes. Advances in Engineering Software, 188:103571, 2024. doi: 10.1016/j.advengsoft.2023.103571.

Matthias Schonlau. Computer experiments and global optimization. PhD thesis, University of Waterloo, Canada, 1997.

Yu Zhang, Zhong-Hua Han, and Ke-Shi Zhang. Variable-fidelity expected improvement method for efficient global optimization of expensive functions. Structural and Multidisciplinary Optimization, 58(4):1431–1451, October 2018. doi: 10.1007/s00158-018-1971-x.